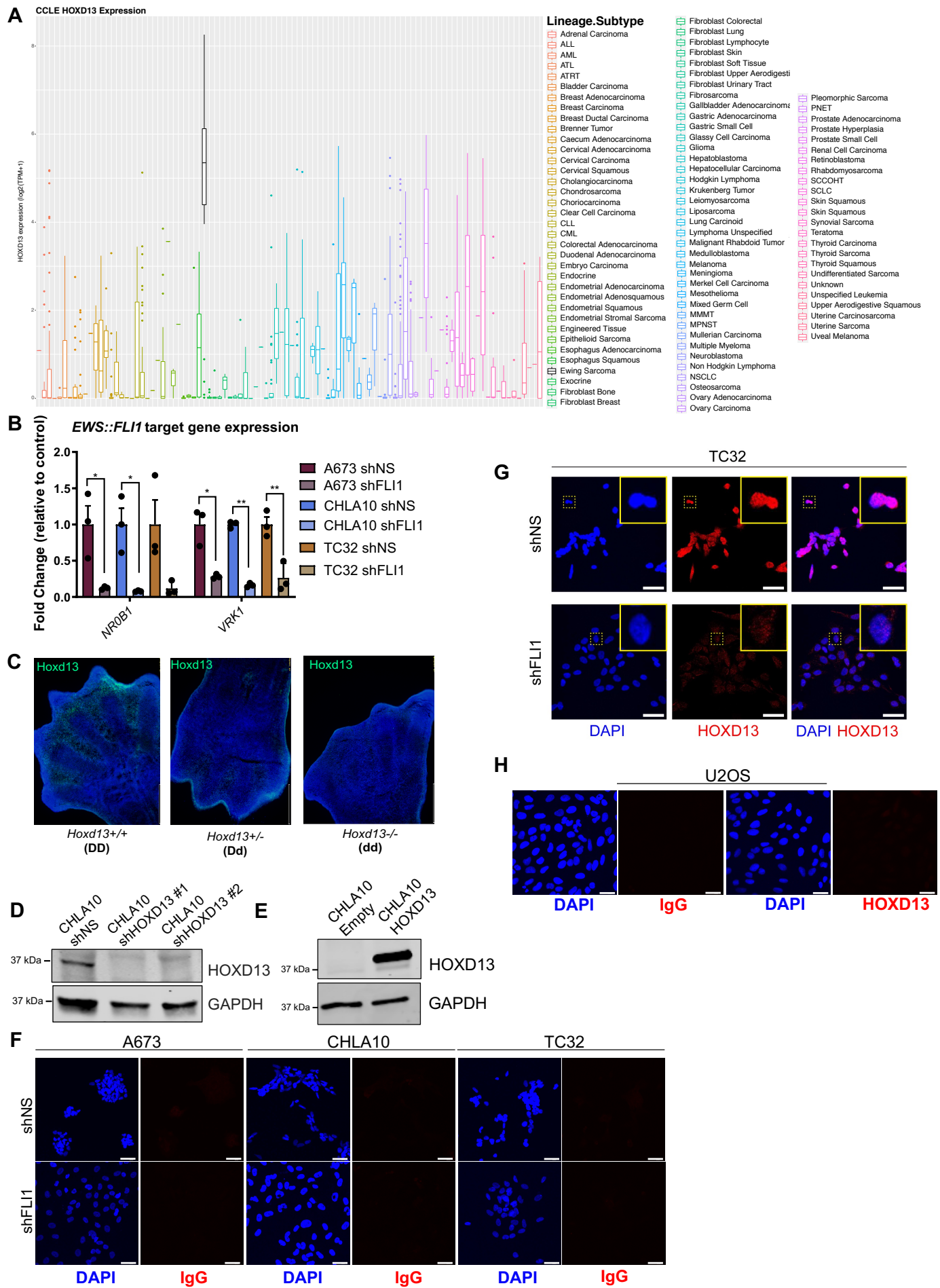


# Supplementary Figures

## Figure S1



**Figure S1. Authentication of EWS::FLI1 knockdown cells and the HOXD13 antibody.** A) *HOXD13* expression across different cell lines grouped by lineage subtype, EwS is in black (32). B) qRT-PCR of EWS::FLI1 target genes, *NR0B1* and *VRK1* after knockdown. Error bars representative of SEM from three independent replicates. \*  $p < 0.05$ ; \*\*  $p < 0.01$ ; Two-way ANOVA; Sidak's multiple comparison test. C) Immunofluorescence detection of Hoxd13 protein expression in distal limbs (autopods) derived from E13.5 *Hoxd13* WT (+/+), het (+/-), or knockout (-/-) mouse embryos. Western blot for HOXD13 after D) knockdown (100ug protein) and E) overexpression (30 ug protein) in CHLA10 cells. F) Fluorescent Immunocytochemistry of HOXD13 (Alexa647) in EWS::FLI1 knockdown cells. Nuclear counterstain was performed with DAPI. Scale bar is 50 um. G-H) Immunofluorescent staining of shFLI1 and U2OS cells with IgG isotype control and HOXD13 antibodies, respectively (secondary antibody Alexa647). Nuclear counterstain was performed with DAPI. Scale bar is 50 um.



**Figure S2. EWS::ETS binding and H3K27ac is conserved across EwS cell lines. A-**  
C) ChIP-seq tracks of EWS::FLI1 binding (blue) and H3K27ac (green) at the PHE of  
EwS cells (34,37). D) ChIP-seq tracks of EWS::ERG binding and H3K27ac at the PHE  
of EwS cells (34,37).



# Figure S3

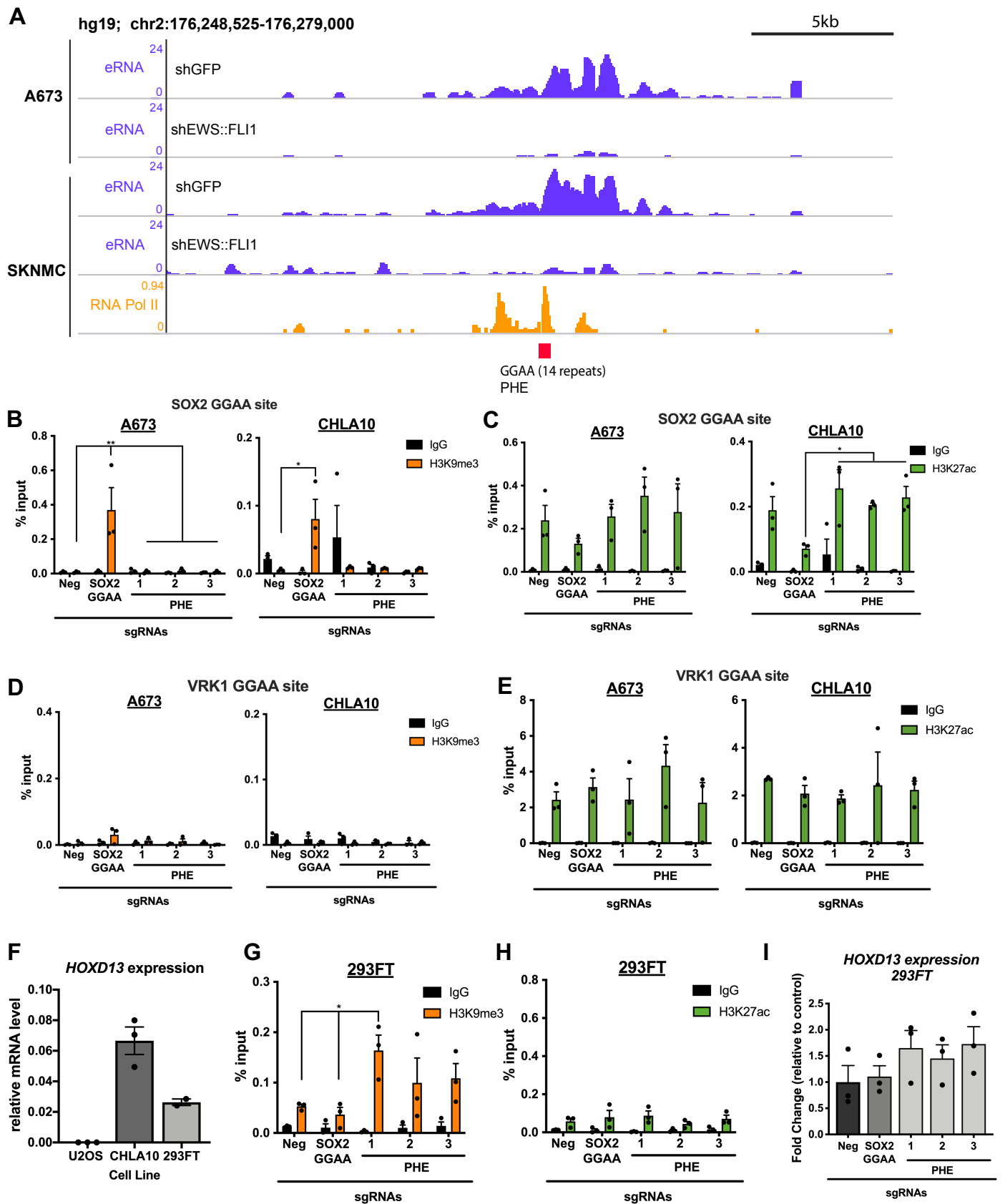


**Figure S3. Enhancer RNA expression at the PHE. A)** NRO-seq tracks of eRNA transcription at the PHE region in A673 and SKNMC cells (6). RNA polymerase II (RNA Pol II) binding at the PHE region in SKNMC cells (ENCODE project GSE32465). CHIP-qPCR for **B)** H3K9me3 and **C)** H3K27ac at the SOX2 GGAA enhancer site. CHIP-qPCR for **D)** H3K9me3 and **E)** H3K27ac at the VRK1 GGAA enhancer site. VRK1 enhancer used as a control GGAA site. **F)** qRT-PCR of baseline *HOXD13* expression in 293FT, U2OS, and CHLA10 cells. CHIP-qPCR for **G)** H3K9me3 and **H)** H3K27ac at the PHE region in gRNA-targeted 293FT cells. **I)** qRT-qPCR of *HOXD13* expression in PHE-targeted 293FT cells. Error bars are representative of SEM from at least three independent experiments. \*  $p < 0.05$ ; \*\*  $p < 0.01$ ; Two tailed t-test; Two-way ANOVA; Sidak's multiple comparison test.

# Figure S4

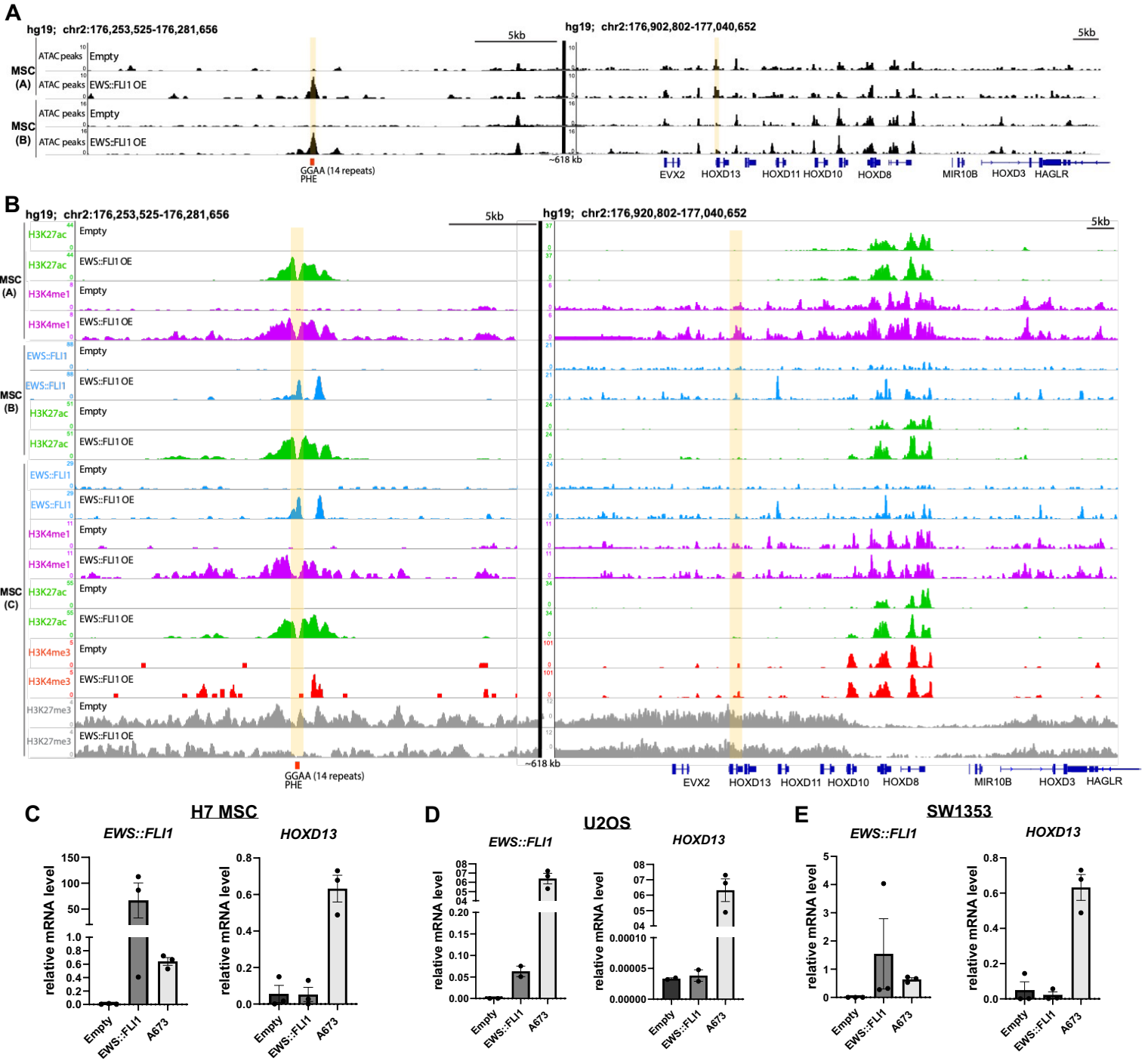
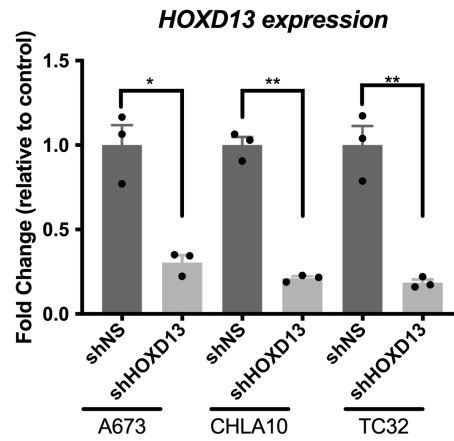


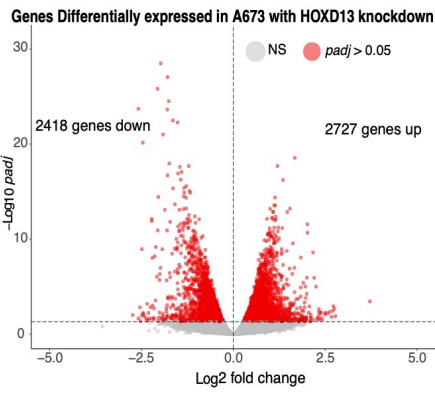
**Figure S4. EWS::FLI1 is not sufficient to induce *HOXD13* transcription in heterologous cell types.** A) ATAC-seq tracks at the PHE and HOXD locus in MSCs transduced with EWS::FLI1 or an empty vector. B) ChIP-seq tracks for EWS::FLI1, H3K27ac, H3K4me1, H3K4me3, and H3K27me3 at the PHE and HOXD locus in MSC's overexpressing EWS::FLI1 or an empty vector. MSC ATAC and ChIP-seq tracks from Refs. (A-C: 2,5,& 6, respectively). qRT-PCR measurement of *EWS::FLI1* and *HOXD13* expression in C) H7 MSCs, D) U20S, and E) SW1353 cells after EWS::FLI1 transduction. A673 cells shown for comparison.

# Figure S5

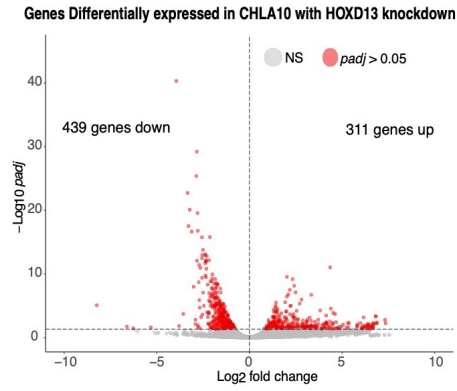
**A**



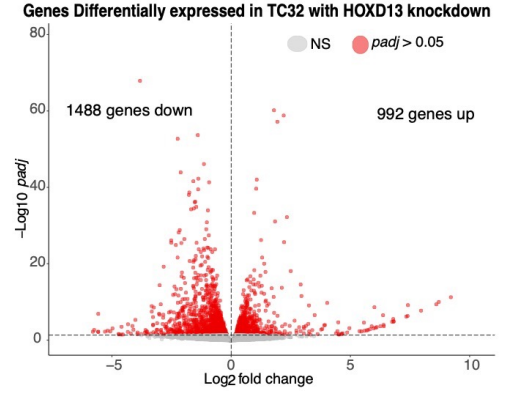
**B**



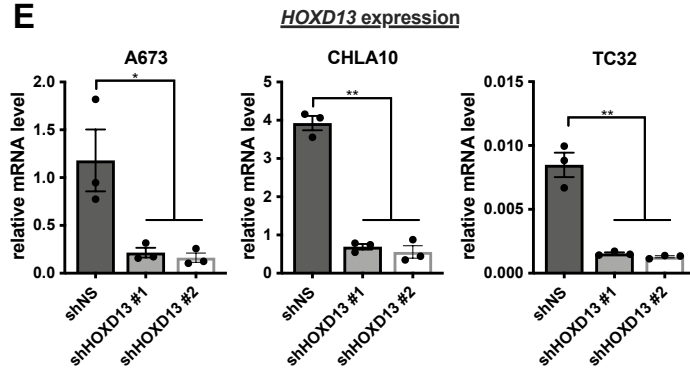
**C**



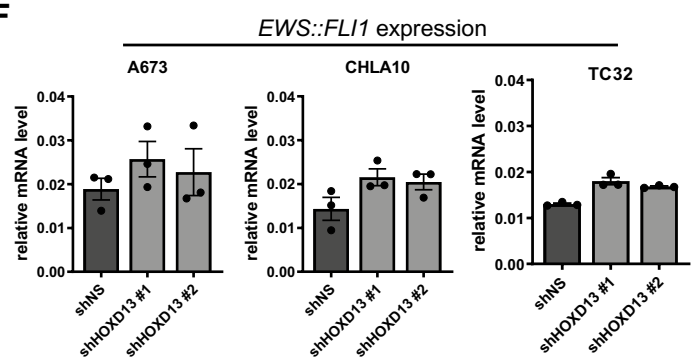
**D**



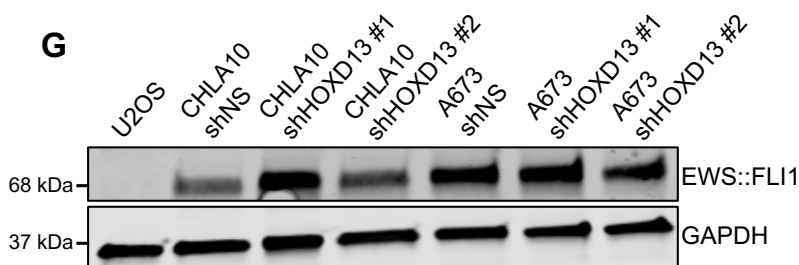
**E**



**F**



**G**



**H**

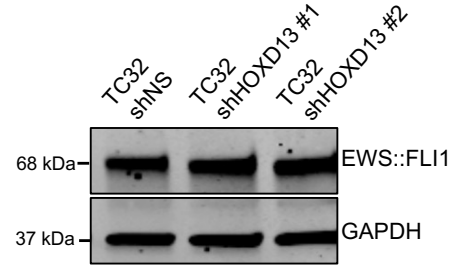


**Figure S5. HOXD13-regulated gene programs are largely cell line-dependent.** A) qRT-PCR of *HOXD13* expression in cells analyzed by RNAseq. B-D) Volcano plots for each cell line depicting the differentially expressed genes after HOXD13 knockdown ( $p_{adj} < 0.05$ ). E) qRT-PCR of *HOXD13* expression of control (shNS) and *HOXD13* (shHOXD13) knockdown cells. F) qRT-PCR of EWS::FLI1 expression in HOXD13 knockdown cells. G-H) Western blot of EWS::FLI1 expression in HOXD13 knockdown cells. Two-tailed *t*-test; One-way ANOVA followed by a Tukey's multiple comparison test. Error bars representative of SEM from three independent replicates. \*  $p < 0.05$ ; \*\*  $p < 0.01$ ; Two-way ANOVA; Sidak's multiple comparison test.



# Figure S6

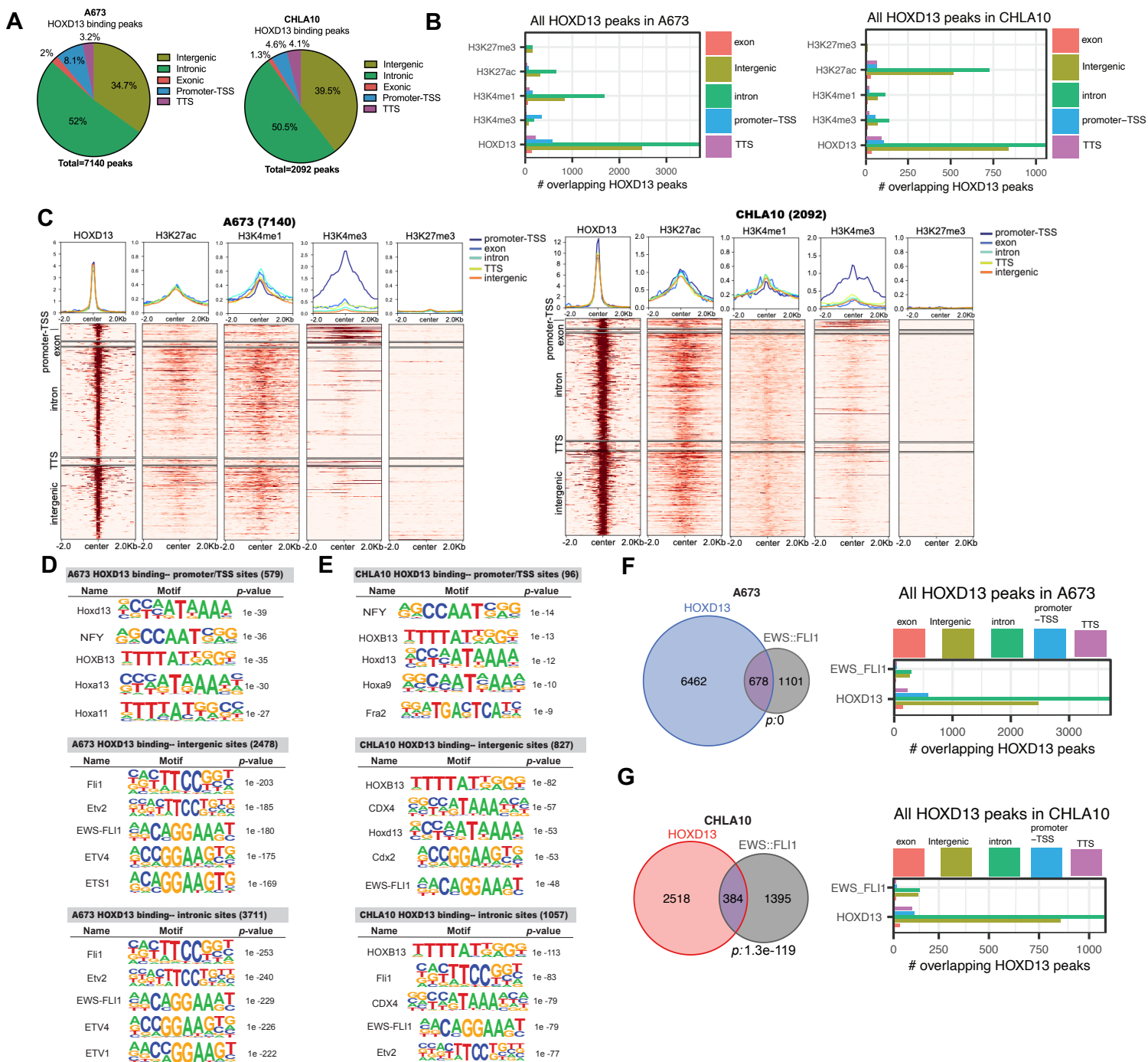


**Figure S6. HOXD13 binding distribution is similar in A673 and CHLA10 cells. A)**

Pie chart showing the genomic distribution HOXD13 binding sites in A673 and CHLA10 cells. B) Bar chart summarizing shared binding sites and associated histone marks at these sites. C) Tornado plots depicting shared HOXD13 binding by genomic location and the associated histone marks at these sites. HOMER Motif analysis by genomic location for the HOXD13 binding sites in D) A673 and E) CHLA10 cells. Venn diagrams showing the overlap between HOXD13 binding sites and published EWS::FLI1 binding sites (2) in F) A673 and G) CHLA10.

# Figure S7

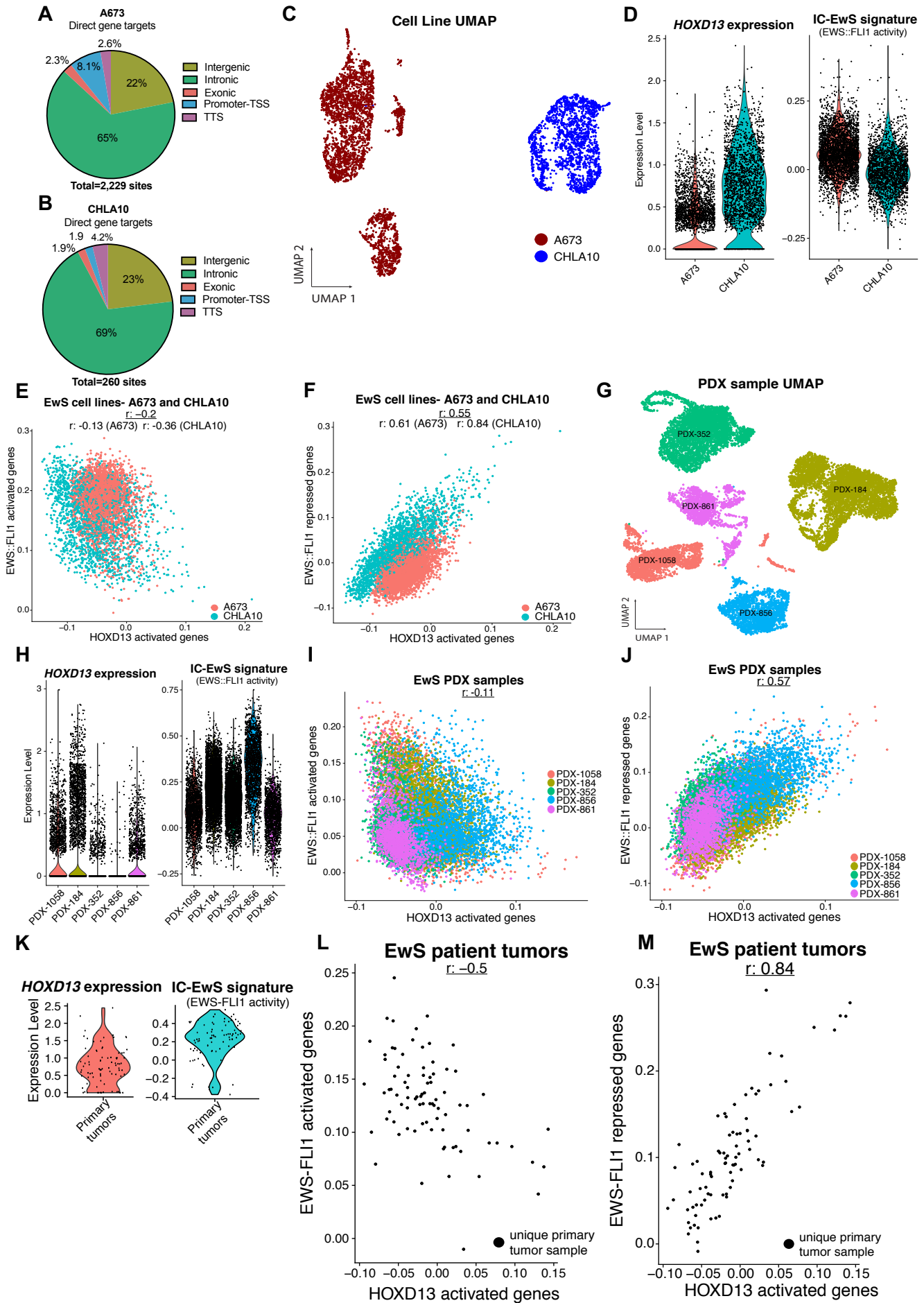


**Figure S7. Single-cell expression of EWS::FLI1 and HOXD13 regulated gene sets.**

**A-B)** Pie charts depict the genomic distribution of these sites. Data were generated using CITE-seq. **C)** Low dimensional embedding, Uniform Manifold Approximation Projection (UMAP), of single-cell gene expression profiles of A673 and CHLA10 cells. **D)** Violin plots showing single-cell HOXD13 expression and the IC-EwS EWS::FLI1 signature in A673 and CHLA10 cells. Scatter plot of HOXD13 activated genes versus **E)** EWS::FLI1 activated genes and **F)** EWS::FLI1 repressed genes by cell line. **G)** Low dimensional embedding, Uniform Manifold Approximation Projection (UMAP), of single-cell gene expression profiles of 5 Ewing sarcoma PDX lines (35). **H)** Violin plots showing single-cell HOXD13 expression and the IC-EwS EWS::FLI1 signature in the PDX lines. Scatter plot of HOXD13 activated genes versus **I)** EWS::FLI1 activated genes and **J)** EWS::FLI1 repressed genes by PDX line. **K)** Violin plots showing HOXD13 expression and the IC-EwS EWS::FLI1 signature in primary tumor samples (n=84). Scatter plot of HOXD13 activated genes versus **L)** EWS::FLI1 activated genes and **M)** EWS::FLI1 repressed genes by primary tumor sample.